



Title	Giant oscillations in spin-dependent tunneling resistances as a function of barrier thickness in fully epitaxial magnetic tunnel junctions with a MgO barrier
Author(s)	Marukame, Takao; Ishikawa, Takayuki; Taira, Tomoyuki; Matsuda, Ken-ichi; Uemura, Tetsuya; Yamamoto, Masafumi
Citation	Physical Review B, 81(13), 134432-1-134432-5 https://doi.org/10.1103/PhysRevB.81.134432
Issue Date	2010-04-27
Doc URL	http://hdl.handle.net/2115/47474
Rights	©2010 The American Physical Society
Type	article
File Information	PRB81(13)_134432.pdf



[Instructions for use](#)

Giant oscillations in spin-dependent tunneling resistances as a function of barrier thickness in fully epitaxial magnetic tunnel junctions with a MgO barrier

Takao Marukame,* Takayuki Ishikawa, Tomoyuki Taira, Ken-ichi Matsuda, Tetsuya Uemura, and Masafumi Yamamoto†
Division of Electronics for Informatics, Hokkaido University, Sapporo 060-0814, Japan

(Received 13 November 2009; revised manuscript received 2 April 2010; published 27 April 2010)

Giant oscillations in spin-dependent tunneling resistances as a function of MgO barrier thickness (t_{MgO}) were observed for fully epitaxial magnetic tunnel junctions with Heusler alloy $\text{Co}_2\text{Cr}_{0.6}\text{Fe}_{0.4}\text{Al}$ electrodes and a MgO barrier. The oscillations in tunneling resistances were well approximated by a superposition of an exponential function of $\exp(at_{\text{MgO}}+b)$ and a periodic function of $1+C\cos[(2\pi/T)t_{\text{MgO}}+\varphi]$ with significantly large amplitudes $C\sim 0.16\pm 0.01$ even at 293 K for both parallel and antiparallel magnetization orientations. The period was found to be almost independent of temperature and bias voltage (V). The amplitudes C showed only weak dependence on V at least up to 0.2 V. These features should be a key to understand the origin of the pronounced oscillations.

DOI: [10.1103/PhysRevB.81.134432](https://doi.org/10.1103/PhysRevB.81.134432)

PACS number(s): 72.25.-b, 73.40.Gk, 75.50.Cc, 85.75.-d

I. INTRODUCTION

Spin-dependent tunneling in magnetic tunnel junctions (MTJs) consisting of epitaxial, single-crystalline ferromagnet/insulator/ferromagnet trilayers has received intensive theoretical and experimental investigation in this decade.¹⁻⁸ The importance of the symmetry of electronic states in the electrodes and of the evanescent states in a single-crystal barrier for spin-dependent tunneling in epitaxial MTJs has been clarified.¹⁻³ This concept combined with atomic-level controlled tunnel barrier preparation technologies resulted in unprecedentedly high tunneling magnetoresistance ratios in fully epitaxial Fe/MgO(001)/Fe MTJs (hereafter, Fe MTJs) (Ref. 7) and related MTJs with a highly oriented MgO barrier and also with highly oriented transition-metal electrodes of $\text{Co}_{1-x}\text{Fe}_x$ (Ref. 8) and CoFeB .⁹ For the complex energy bands in a single-crystal MgO barrier, Butler *et al.* theoretically predicted a quantum interference effect between the evanescent states in the single-crystal MgO barrier.² Yuasa *et al.* reported an oscillation in the tunneling magnetoresistance (TMR) ratio as a function of the MgO barrier thickness (t_{MgO}) for epitaxial Fe MTJs at 20 and 293 K.⁷ Later, Matsumoto *et al.* reported oscillations in the tunneling resistances R_{P} and R_{AP} for the parallel (P) and antiparallel (AP) magnetization orientations between the lower and upper electrodes, respectively, as a function of t_{MgO} at 20 K for Fe MTJs.¹⁰ They reported an oscillation with a short period of 0.32 nm for R_{P} and an oscillation expressed as a superposition of a short period of 0.32 nm and a long period of 0.99 nm for R_{AP} . Matsumoto *et al.* discussed a possible origin based on the quantum interference effect of evanescent states in a MgO barrier predicted by Butler *et al.*, in particular, through possible contributions of hot spots for both P and AP but the origin has not been understood yet.¹⁰

Our purpose in the present study has been to investigate possible oscillations in R_{P} and R_{AP} in MgO-based MTJs with different electrodes and clarify the factors that affect the oscillations. The investigation and clarification are essential not only for the understanding of the physics behind the oscillations in MTJs but also for the creation of future-generation spintronic devices based on a novel operating principle. A

possible candidate is a combination of Co-based Heusler alloys (Co_2YZ , where Y is usually a transition metal and Z is a main group element) (Ref. 11) and a MgO barrier. We recently proposed and developed fully epitaxial MTJs with Co_2YZ electrodes¹²⁻¹⁶ and a MgO barrier to thoroughly utilize the potentially high spin polarization of this material system.¹⁷⁻²⁰ We have observed oscillations in the TMR ratio as a function of t_{MgO} for fully epitaxial MgO-based MTJs with Heusler alloy Co_2MnSi thin films as both lower and upper electrodes, $\text{Co}_2\text{MnSi}/\text{MgO}/\text{Co}_2\text{MnSi}$ MTJs (Co_2MnSi MTJs), with a period of 0.28 nm.²¹ The oscillation period of 0.28 nm was close to the short oscillation period of 0.32 nm for the oscillatory t_{MgO} dependence of R_{P} and R_{AP} observed for Fe MTJs. However, we could not extract the oscillatory components of R_{P} and R_{AP} for the fabricated Co_2MnSi MTJs because possible oscillations in R_{P} and/or R_{AP} were veiled by the scattering of the junction area. On the other hand, the junction area scattering does not affect the TMR ratio because the TMR ratio calculated as $(R_{\text{AP}}-R_{\text{P}})/R_{\text{P}}$ is independent of the junction area.

Among several combinations of Co_2YZ and a MgO barrier, $\text{Co}_2\text{Cr}_{0.6}\text{Fe}_{0.4}\text{Al}$ (CCFA) features a smaller lattice mismatch with MgO(001) of -3.7% for a 45° in-plane rotation within the (001) plane,¹² which is a contrast to that of -5.1% between $\text{Co}_2\text{MnSi}(001)$ and MgO and also lower than that of -3.9% between Fe(001) and MgO. We have demonstrated extremely smooth and abrupt interfaces in (from the lower electrode side) CCFA/MgO(001)/ $\text{Co}_{50}\text{Fe}_{50}$ (CoFe) fully epitaxial MTJ trilayers and measured a relatively high TMR ratio of 317% at 4.2 K (109% at room temperature) for CCFA/MgO/CoFe MTJs.¹⁴

Given this background, we investigated possible oscillations in fully epitaxial MTJs with a single-crystal MgO(001) barrier and Heusler alloy CCFA as both lower and upper electrodes CCFA/MgO(001)/CCFA MTJs (hereafter, CCFA MTJs). We found pronounced oscillatory behaviors for R_{P} and R_{AP} for CCFA MTJs with large oscillation amplitudes that were about eight times greater even at 293 K than those observed for Fe MTJs at 20 K.¹⁰ Thus, we unambiguously demonstrated the existence of oscillations in R_{P} and R_{AP} as a function of the barrier thickness.

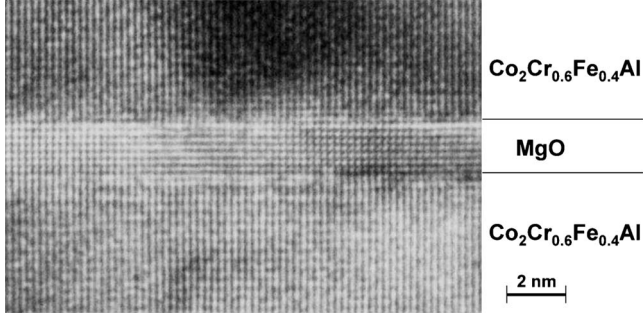


FIG. 1. Cross-sectional high-resolution transmission electron microscope lattice image of a fabricated CCFA/MgO (2.0 nm)/CCFA MTJ layer structure, along the $[1-10]$ direction of the CCFA layers.

II. EXPERIMENTAL

The fabricated CCFA-MTJ layer structure was as follows: (from the substrate side) MgO buffer (10 nm)/lower CCFA (50 nm)/MgO (0.8–3.4 nm)/upper CCFA (10 nm)/Ru (0.8 nm)/Co₉₀Fe₁₀ (2 nm)/IrMn (10 nm)/Ru cap (5 nm), grown on MgO(001) substrates.²² The preparation of the fully epitaxial CCFA MTJs is described in detail elsewhere.²² The nominal thickness of the MgO tunnel barrier (t_{MgO}) was varied from 0.8 to 3.4 nm on each $20 \times 20 \text{ nm}^2$ substrate by a linearly moving shutter during the deposition by electron-beam evaporation. We fabricated densely arranged MTJs with the fully epitaxial layer structure through photolithography. The fabricated junction size was $10 \times 10 \text{ }\mu\text{m}^2$ or $8 \times 8 \text{ }\mu\text{m}^2$. The magnetoresistance was measured using a dc four-probe method with a magnetic field applied along the $[110]$ axis of the CCFA. The bias voltage (V) was defined with respect to the lower electrode. For comparison, we also identically fabricated densely arranged fully epitaxial CCFA/MgO/CoFe MTJs with the nominal t_{MgO} ranging from 0.8 to 3.4 nm. The fabricated CCFA/MgO/CoFe MTJ layer structure was essentially the same as the CCFA-MTJ layer structure described above except that the upper electrode was replaced by a CoFe electrode (3 nm). We measured R_{P} and R_{AP} as a function of t_{MgO} for CCFA MTJs at 4.2 and 293 K and for CCFA/MgO/CoFe MTJs at 293 K.

III. RESULTS AND DISCUSSION

A cross-sectional high-resolution transmission electron microscope lattice image of a fabricated CCFA/MgO/CCFA MTJ layer structure is shown in Fig. 1. This image clearly shows that all the layers of the CCFA-MTJ trilayer were grown epitaxially and were single crystalline. It also confirms that extremely smooth and abrupt interfaces were formed.

We will now describe the t_{MgO} dependence of R_{P} and R_{AP} . Figures 2(a) and 2(b) show $R_{\text{P}}A$ and $R_{\text{AP}}A$ as a function of t_{MgO} at 4.2 K and 293 K, respectively, along with the corresponding TMR ratios in (c), for fully epitaxial CCFA MTJs, where A represents the nominal junction area. Pronounced oscillatory dependences were observed in both $\ln R_{\text{P}}$ vs t_{MgO} and $\ln R_{\text{AP}}$ vs t_{MgO} plots at 4.2 and 293 K, as shown in Figs.

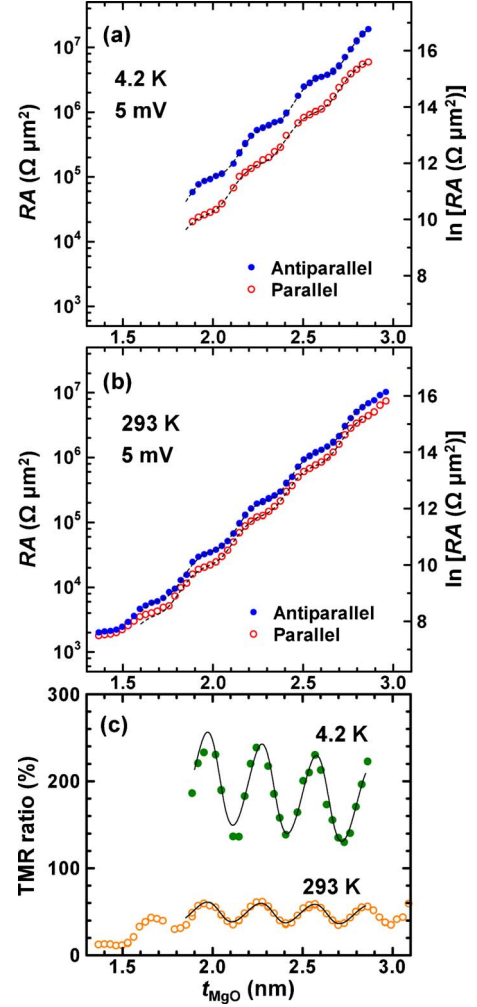


FIG. 2. (Color online) Closed and open circles represent $R_{\text{AP}}A$ and $R_{\text{P}}A$, respectively, as a function of t_{MgO} at (a) 4.2 K and (b) 293 K for fully epitaxial CCFA/MgO/CCFA MTJs, where R_{P} and R_{AP} are respective tunnel resistances for the P and AP magnetization orientations and A is the nominal junction area of $10 \times 10 \text{ }\mu\text{m}^2$. The bias voltage was 5 mV. Each dashed line is a curve fitted with Eq. (2) described in the text. (c) Closed and open circles represent corresponding experimental TMR ratios defined as $(R_{\text{AP}} - R_{\text{P}})/R_{\text{P}}$ as a function of t_{MgO} at 4.2 K and 293 K calculated from the experimental R_{P} and R_{AP} values shown in (a) and (b), respectively. The solid curves are the values of the TMR ratios calculated using the approximate functions for R_{P} and R_{AP} as a function of t_{MgO} with Eq. (2).

2(a) and 2(b). These clear periodic behaviors in $\ln R$ vs t_{MgO} plots for both P and AP for both 4.2 and 293 K are characterized by the alternate appearance of two regions in each period: one with a gentle slope α_L and the other with a steep slope α_H in both $\ln R$ vs t_{MgO} .

To extract characteristic features of these distinct periodic behaviors, we first approximated the baseline dependence of R_{P} (R_{AP}) by an exponential function $\exp(at_{\text{MgO}} + b)$ for a t_{MgO} range from 1.7 to 3.0 nm for 293 K and from 1.9 to 2.85 nm for 4.2 K by the least-squares method. Then, we analyzed the reduced tunnel resistance r_{P} (r_{AP}), which is tunnel resistance R_{P} (R_{AP}) divided by each baseline function $\exp(at_{\text{MgO}} + b)$.

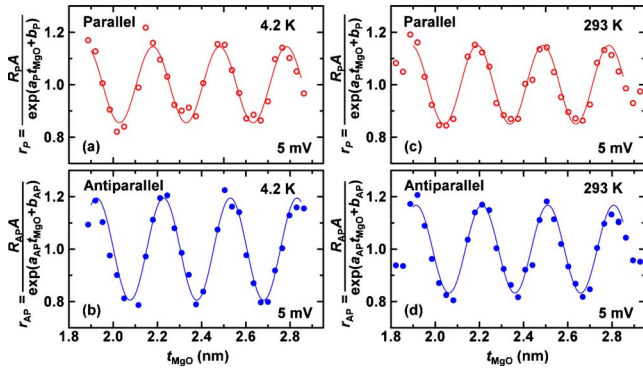


FIG. 3. (Color online) Open and closed circles represent reduced tunnel resistances r_P and r_{AP} , respectively, at 4.2 and 293 K for CCFA MTJs (the same MTJs as for Fig. 2), where r_P (r_{AP}) is the tunnel resistance R_{PA} (R_{AP}) divided by each baseline function of $\exp(at_{MgO}+b)$. The R_{PA} and R_{AP} values are the same as for Fig. 2. (a) and (b) r_P and r_{AP} at 4.2 K. (c) and (d) r_P and r_{AP} at 293 K. Each solid line is a fitted curve with a form of $r=1+C \cos[(2\pi/T)t_{MgO}+\varphi]$.

We then approximated r_P and r_{AP} at 4.2 and 293 K by

$$r = 1 + C \cos[(2\pi/T)t_{MgO} + \varphi] \quad (1)$$

with three parameters: oscillation amplitude C , period T , and phase φ (the first step of the approximation for r_P and r_{AP}). The periods thus obtained for P and AP and for 4.2 and 293 K agreed well each other and were $0.30 \text{ nm} \pm 2\%$. The difference of $\pm 2\%$ is negligible. Thus, we conclude that the periods are common for P and AP and independent of temperature, at least up to 293 K. The period of 0.30 nm obtained for CCFA MTJs is in good agreement with the period of 0.32 nm observed for the short-period oscillations in r_P and r_{AP} for Fe MTJs. Although both r_P and r_{AP} were well approximated by the first-step approximation with the three fitting parameters for each r_P or r_{AP} , we again fitted the oscillations in r_P and r_{AP} with Eq. (1) with the thus-obtained common period of 0.30 nm (the second step of the approximation for r_P and r_{AP}) to obtain more certain phase difference values of $\varphi_P - \varphi_{AP}$. (The amplitudes C_P and C_{AP} obtained by the second-step approximation were almost equal to those obtained by the first-step approximation.) The solid lines for r_P and r_{AP} shown in Fig. 3 are curves fitted in this manner. Both r_P and r_{AP} were well approximated by Eq. (1) at both 4.2 and 293 K.

Note that the oscillations in both r_P and r_{AP} for CCFA MTJs were well approximated by a single period of 0.30 nm. This is a contrast to the more complex oscillatory dependence of r_{AP} for Fe MTJs expressed by a superposition of a short-period oscillation and a long-period oscillation described above. The period of 0.30 nm observed for CCFA MTJs is close to that of 0.32 nm for oscillations observed in Fe MTJs. The period of 0.30 nm is independent of the MgO(001) interplanar distance (0.21 nm), as in the case for Fe MTJs.¹⁰

Notably large oscillation amplitudes for P and AP, C_P and C_{AP} , respectively, were observed for both 4.2 K and 293 K for CCFA MTJs. The values of C_P and C_{AP} obtained by

fitting were 0.17 ± 0.02 ($C_P=0.154$ and $C_{AP}=0.193$) at 4.2 K and 0.16 ± 0.01 ($C_P=0.149$ and $C_{AP}=0.168$) at 293 K. Thus, we conclude that (1) the oscillation amplitudes C in the reduced tunnel resistances r_P and r_{AP} were almost independent of temperature, at least up to 293 K, and (2) there was no significant difference in C_P and C_{AP} , although C_{AP} was 1.25 and 1.13 times larger than C_P at 4.2 and 293 K, respectively. Note that these values of C_P and C_{AP} are significantly large, and are about eight times those of about 0.02 observed for oscillations in r_P and r_{AP} for Fe MTJs at 20 K.¹⁰

Note that in Fig. 3 there is no background variation in the r_P vs t_{MgO} and r_{AP} vs t_{MgO} plots from the oscillatory dependences expressed as $r=1+C \cos[(2\pi/T)t_{MgO}+\varphi]$ at both 4.2 and 293 K, which is a contrast to significant background variations in the r_P vs t_{MgO} and r_{AP} vs t_{MgO} plots observed for Fe MTJs.¹⁰ This means that R_P (R_{AP}) is well approximated by the simple product of two terms without any corrections: the first is the baseline function $\exp(at_{MgO}+b)$ and the second is the periodic function $1+C \cos[(2\pi/T)t_{MgO}+\varphi]$. Thus, R_{PA} and R_{AP} are well approximated by

$$RA = [\exp(at_{MgO}+b)][1+C \cos[(2\pi/T)t_{MgO}+\varphi]], \quad (2)$$

at both 4.2 and 293 K [Figs. 2(a) and 2(b)]. This expression provides approximate slopes $\alpha_L = a - (2\pi/T)C\gamma$ and $\alpha_H = a + (2\pi/T)C\gamma$ for the gentle and steep slope regions, respectively, in the $\ln R$ vs t_{MgO} plots for both P and AP. Here, γ is a numerical factor of about 0.78 associated with the approximation. Thus, the pronounced periodic dependences observed for $\ln R$ vs t_{MgO} plots for P and AP [Figs. 2(a) and 2(b)] are due to the large C_P and C_{AP} values for CCFA MTJs.

Oscillations in r_P and r_{AP} showed phase differences $\varphi_P - \varphi_{AP}$ of ~ 0.16 and 0.07 times the period of 0.30 nm at 4.2 and 293 K, respectively. This temperature dependence of $\varphi_P - \varphi_{AP}$ was mainly caused by the temperature dependence of φ_{AP} .

Closed and open circles in Fig. 2(c) show the corresponding experimental TMR ratios defined as $(R_{AP}-R_P)/R_P$ as a function of t_{MgO} at 4.2 and 293 K calculated from the experimental R_P and R_{AP} values shown in Figs. 2(a) and 2(b), respectively. Because of the oscillations in R_P and R_{AP} , the TMR ratios (α) showed clear oscillations with typical peak and valley α values of $\alpha_{\text{peak}}=238\%$ and $\alpha_{\text{valley}}=136\%$ at 4.2 K ($\alpha_{\text{peak}}:\alpha_{\text{valley}}=1:0.57$ or $\alpha_{\text{peak}}/\alpha_{\text{valley}}=1.75$) and $\alpha_{\text{peak}}=60\%$ and $\alpha_{\text{valley}}=38\%$ at 293 K ($\alpha_{\text{peak}}:\alpha_{\text{valley}}=1:0.63$ or $\alpha_{\text{peak}}/\alpha_{\text{valley}}=1.58$). The solid curves in Fig. 2(c) are the TMR ratios calculated using the approximate functions for R_P and R_{AP} as a function of t_{MgO} with Eq. (2). Of course, the curves thus calculated well reproduce the experimental TMR ratios. This is because the experimental TMR ratios and the curves were both basically derived from the same experimental R_P and R_{AP} values: the experimental TMR ratios were calculated using the experimental R_P and R_{AP} directly, while the curves were calculated using the approximate functions of experimental R_P and R_{AP} as a function of t_{MgO} with Eq. (2).

Figures 4(a) and 4(b) show r_P and r_{AP} as a function of t_{MgO} at 293 K for various positive V up to 0.2 V for a different set of CCFA MTJs from those shown in Figs. 2 and 3 but fabricated in the same preparation run on the same 20

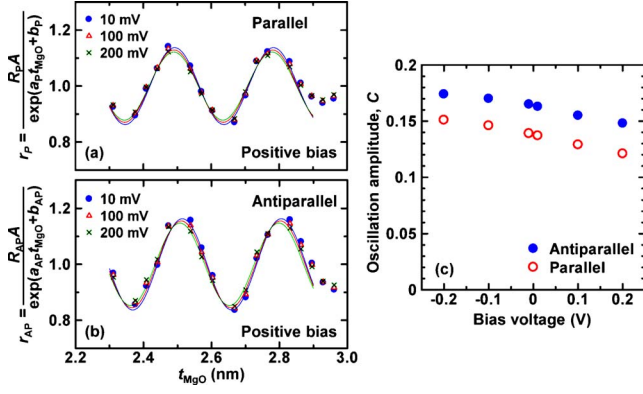


FIG. 4. (Color online) Closed circles, open triangles, and crosses represent reduced tunnel resistances r_P and r_{AP} as a function of t_{MgO} at 293 K for various positive V up to 0.2 V for a different set of CCFA MTJs from those shown in Fig. 2. (a) and (b) r_P and r_{AP} for positive V up to 0.2 V, respectively. Solid lines are curves fitted with Eq. (1). (c) Oscillation amplitudes for P (open circles) and AP (closed circles) [C_P and C_{AP} in Eq. (1)] as a function of V from -0.2 to 0.2 V. The bias voltage was defined with respect to the lower CCFA electrode. Here, the junction size was $8 \times 8 \mu\text{m}^2$.

$\times 20$ nm MgO substrate. Clear oscillations in r_P and r_{AP} were observed for V up to 0.2 V for both polarities. The solid lines in Fig. 4 are curves fitted using Eq. (1). The fitting results showed periods $T \sim 0.29 \text{ nm} \pm 0.3\%$ for both P and AP for both polarities up to ± 0.2 V, which were in good agreement with $T \sim 0.30 \text{ nm} \pm 2\%$ observed for the MTJs shown in Fig. 3 (the slight difference in T of 3.0% may suggest a small inhomogeneity in t_{MgO} along the direction perpendicular to the wedge direction on a substrate). Figure 4(c) shows the oscillation amplitudes C_P and C_{AP} as a function of V from -0.2 to 0.2 V, obtained by fitting, which demonstrates that C_{AP} is slightly larger than C_P . Importantly, both C_P and C_{AP} showed weak dependence on V up to ± 0.2 V. However, in more detail, they decreased by 20% and 15% with increasing V from -0.2 V to 0.2 V, respectively. This asymmetric dependence on the bias polarity suggests that the possible difference in the bulk states or interface states of the lower and upper CCFA electrodes affects the oscillation amplitude.

We also found clear oscillations in R_P and R_{AP} as a function of t_{MgO} for identically fabricated CCFA/MgO/CoFe MTJs at 293 K [Fig. 5(a)]. The oscillations in the reduced resistances r_P and r_{AP} [Figs. 5(b) and 5(c)] were also well approximated by Eq. (1) with respective parameters and without any background correction, as in the case of CCFA MTJs. The periods, T_P and T_{AP} , are also nearly equal and are $0.31 \text{ nm} \pm 2\%$. Thus, the periods were also close to those observed for CCFA MTJs and Fe MTJs.¹⁰ Note that the amplitudes, C_P and C_{AP} , observed for CCFA/MgO/CoFe MTJs were $0.053 \pm 12\%$. These values are about 1/3 of those observed for CCFA MTJs but still about three times those observed for Fe MTJs. Oscillations in r_P and r_{AP} showed a phase difference $\varphi_P - \varphi_{AP}$ of ~ 0.09 times the period of 0.31 nm at 293 K for CCFA/MgO/CoFe MTJs. This phase difference is close to that of ~ 0.07 times the period of 0.30 nm at 293 K for CCFA MTJs.

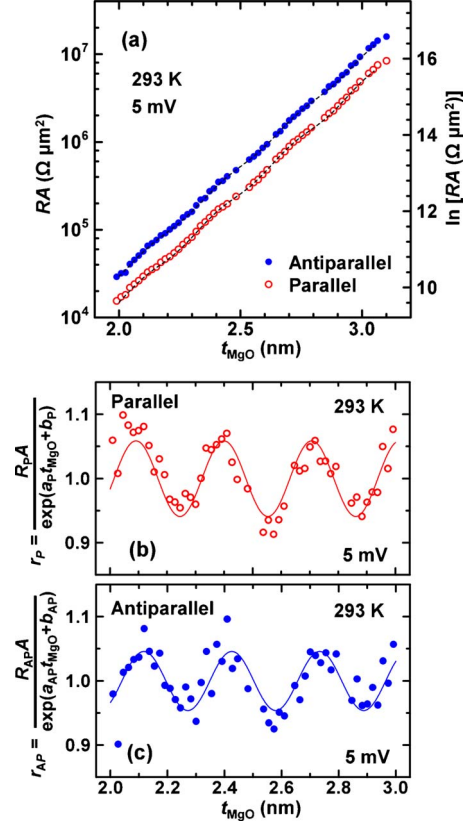


FIG. 5. (Color online) (a) Closed and open circles represent $R_{AP}A$ and R_PA , respectively, as a function of t_{MgO} at 293 K for fully epitaxial CCFA/MgO/CoFe MTJs, where R_P and R_{AP} are respective tunnel resistances for the P and AP magnetization orientations, and A is the nominal junction area of $10 \times 10 \mu\text{m}^2$. The bias voltage was 5 mV. Each dashed line is a curve fitted with Eq. (2) described in the text with respective parameters and without any background correction. (b) and (c) Open and closed circles represent reduced tunnel resistances r_P and r_{AP} , respectively, at 293 K, where r_P (r_{AP}) is the tunnel resistance R_{PA} (R_{APA}) divided by each baseline function of $\exp(at_{MgO}+b)$. The R_{PA} and R_{APA} values are the same as for Fig. 5(a). Each solid line is a curve fitted with Eq. (1) with respective parameters.

We will now discuss whether our experimental findings can be explained by the quantum interference of evanescent states in the MgO barrier proposed by Butler *et al.*² This model takes into account quantum interference of two wave functions having respective complex perpendicular wave-vector components k_z with finite real-part values $k_{r1} \neq k_{r2}$ and the same imaginary part κ , resulting in a transmittance given by $[\exp(-2\kappa t_{MgO})][1 + \cos[k_{r1} - k_{r2}]t_{MgO}]$, a damped oscillatory function with respect to t_{MgO} . This function provides a period $T = 2\pi / (k_{r1} - k_{r2})$ for a given pair of $k_{z1} = k_{r1} + i\kappa$ and $k_{z2} = k_{r2} + i\kappa$. However, the model cannot provide a uniquely determined period for the tunneling current oscillations. In addition, our experimental finding of the constant period with respect to temperature and V up to ± 0.2 V for both P and AP is hard to attribute to the model proposed by Butler *et al.* In particular, the constant single period observed even for the increased V up to ± 0.2 V is hard to discuss on the basis of this model.

Furthermore, this model considers only the quantum interference effect within the MgO barrier. However, the experimental findings clearly demonstrate that (1) the oscillation amplitude is strongly dependent on the choice of ferromagnetic electrode materials and (2) it is also influenced by the possible difference in the bulk states or interface states of the lower and upper electrodes. Therefore, the bulk and/or interface states should be taken into consideration along with the complex energy band in the MgO barrier. Although it is beyond the scope of the present study, the investigation of the electronic and magnetic states and microscopic structural properties for the interfacial regions between ferromagnetic electrodes and a MgO barrier is particularly important to reveal the origin of the observed pronounced oscillations. Our experimental findings that (1) the periods and amplitudes are almost identical for both P and AP, (2) the periods are almost independent of temperature and V , and (3) the oscillation amplitudes show only weak dependence on V suggest that all electrons contributing to tunneling are influenced by a certain effect, which varies periodically with t_{MgO} with the period of ~ 0.30 nm.

IV. SUMMARY

In summary, we unambiguously demonstrated pronounced oscillations in R_P and R_{AP} with t_{MgO} for fully epitaxial MgO-based MTJs with Heusler alloy $\text{Co}_2\text{Cr}_{0.6}\text{Fe}_{0.4}\text{Al}$ as both the lower and upper electrodes. The period of oscillations was almost independent of temperature up to 293 K and bias voltage V up to 0.2 V and the amplitude showed only weak dependence on V up to 0.2 V. These experimental findings should be a key to understand the origin of the oscillations.

ACKNOWLEDGMENTS

We thank S. Yuasa, M. Shirai, J. Inoue, and S. Blügel for valuable discussions. This work was partly supported by Grants-in-Aid for Scientific Research (A) (Grant No. 20246054) and (B) (Grant No. 21360140), and a Grant-in-Aid for Scientific Research on Priority Area "Creation and Control of Spin Current" (Grant No. 19048001) from MEXT, Japan.

*Present address: Corporate R&D Center, Toshiba Corp., Kawasaki 212-8582, Japan.

†yamamoto@nano.ist.hokudai.ac.jp

¹Ph. Mavropoulos, N. Papanikolaou, and P. H. Dederichs, *Phys. Rev. Lett.* **85**, 1088 (2000).

²W. H. Butler, X.-G. Zhang, T. C. Schulthess, and J. M. MacLaren, *Phys. Rev. B* **63**, 054416 (2001).

³J. Mathon and A. Umerski, *Phys. Rev. B* **63**, 220403(R) (2001).

⁴W. Wulfhekel, M. Klaua, D. Ullmann, F. Zavaliche, J. Kirschner, R. Urban, T. Monchesky, and B. Heinrich, *Appl. Phys. Lett.* **78**, 509 (2001).

⁵M. Bowen, V. Cros, F. Petroff, A. Fert, C. Martínez Boubeta, J. L. Costa-Krämer, J. V. Anguita, A. Cebollada, F. Briones, J. M. de Teresa, L. Morellón, M. R. Ibarra, F. Güell, F. Peiró, and A. Cornet, *Appl. Phys. Lett.* **79**, 1655 (2001).

⁶J. Faure-Vincent, C. Tiusan, E. Jouguelet, F. Canet, M. Sajjiedine, C. Bellouard, E. Popova, M. Hehn, F. Montaigne, and A. Schuhl, *Appl. Phys. Lett.* **82**, 4507 (2003).

⁷S. Yuasa, T. Nagahama, A. Fukushima, Y. Suzuki, and K. Ando, *Nat. Mater.* **3**, 868 (2004).

⁸S. S. P. Parkin, C. Kaiser, A. Panchula, P. M. Rice, B. Hughes, M. Samant, and S.-H. Yang, *Nat. Mater.* **3**, 862 (2004).

⁹D. D. Djayaprawira, K. Tsunekawa, M. Nagai, H. Maehara, S. Yamagata, N. Watanabe, S. Yuasa, Y. Suzuki, and K. Ando, *Appl. Phys. Lett.* **86**, 092502 (2005).

¹⁰R. Matsumoto, A. Fukushima, T. Nagahama, Y. Suzuki, K.

Ando, and S. Yuasa, *Appl. Phys. Lett.* **90**, 252506 (2007).

¹¹C. Felser, G. H. Fecher, and B. Balke, *Angew. Chem., Int. Ed.* **46**, 668 (2007).

¹²T. Marukame, T. Kasahara, K.-i. Matsuda, T. Uemura, and M. Yamamoto, *Jpn. J. Appl. Phys., Part 2* **44**, L521 (2005).

¹³T. Ishikawa, T. Marukame, H. Kijima, K.-i. Matsuda, T. Uemura, M. Arita, and M. Yamamoto, *Appl. Phys. Lett.* **89**, 192505 (2006).

¹⁴T. Marukame, T. Ishikawa, S. Hakamata, K.-i. Matsuda, T. Uemura, and M. Yamamoto, *Appl. Phys. Lett.* **90**, 012508 (2007).

¹⁵T. Ishikawa, N. Itabashi, T. Taira, K.-i. Matsuda, T. Uemura, and M. Yamamoto, *J. Appl. Phys.* **105**, 07B110 (2009).

¹⁶M. Yamamoto, T. Ishikawa, T. Taira, G.-f. Li, K.-i. Matsuda, and T. Uemura, *J. Phys.: Condens. Matter* **22**, 164212 (2010).

¹⁷S. Ishida, S. Fujii, S. Kashiwagi, and S. Asano, *J. Phys. Soc. Jpn.* **64**, 2152 (1995).

¹⁸S. Picozzi, A. Continenza, and A. J. Freeman, *Phys. Rev. B* **66**, 094421 (2002).

¹⁹I. Galanakis, P. H. Dederichs, and N. Papanikolaou, *Phys. Rev. B* **66**, 174429 (2002).

²⁰Y. Miura, K. Nagao, and M. Shirai, *Phys. Rev. B* **69**, 144413 (2004).

²¹T. Ishikawa, S. Hakamata, K.-i. Matsuda, T. Uemura, and M. Yamamoto, *J. Appl. Phys.* **103**, 07A919 (2008).

²²T. Marukame, T. Ishikawa, S. Hakamata, K.-i. Matsuda, T. Uemura, and M. Yamamoto, *IEEE Trans. Magn.* **43**, 2782 (2007).